Supplemental Information

USP9X deubiquitinates ALDH1A3 and maintains mesenchymal identity in glioblastoma stem cells

Zhengxin Chen, Hong-Wei Wang, Shuai Wang, Ligang Fan, Shuang Feng, Xiaomin Cai, Chenghao Peng, Xiaoting Wu, Jiacheng Lu, Dan Chen, Yuanyuan Chen, Wenting Wu, Daru Lu, Ning Liu, Yongping You, Huibo Wang

Supplemental Figure 1. USP9X maintains ALDH1A3 stability

(A) IB analysis of ALDH1A3 expression in HEK293T cells and NHAs after treatment with 100 μg/ml CHX or 20 μM MG132. **(B)** A siGENOME RTF library targeting 98 known DUBs identified four candidates, when knocked down in HEK293T cells, decreased ALDH1A3 protein levels. Red arrow indicates USP9X. **(C)** IB analysis of USP9X and ALDH1A3 levels in U87MG and T98G GBM cell lines transduced with USP9X siRNA or control siRNA. **(D)** qRT-PCR analysis of ALDH1A3 mRNA expression in HEK293T cells and NHAs after transduction with vector control or Flag-USP9X. **(E)** qRT-PCR analysis of ALDH1A3 mRNA expression in U87MG and T98G GBM cell lines depleted of USP9X. **(F** and **G)** FACS sorting of $CD44^-$ and $CD44^+$ subpopulations from primary GBM 21 and GBM 505 cells **(F)**, as well as $CD133^-$ and $CD133^+$ subpopulations from primary GBM 35 and GBM 182 cells **(G)**. **(H** and **I)** Representative images of $CD44^+$ cell **(H)** or $CD133^+$ cell **(I)**-derived tumorspheres cultured in serum-free medium, and $CD44^-$ or $CD133^-$ cells cultured in serum. **(J** and **K)** FACS analysis of two MES GSCs (MES 21 and 505) based on CD44 and ALDH1 expression **(J)**, as well as two PN GSCs (PN 35 and 182) based on CD133 and CD15 expression **(K)**. **(L** and **M)** IF images of CD44 and OLIG2 expression in MES 21 and 505 GSCs **(L)**, as well as PN 35 and 182 GSCs **(M)**. CD44 was labeled in red. OLIG2 was labeled in green. Nuclei were counterstained with DAPI (blue). **(N)** Representative images of MES 21, MES 505, PN 35 and 182 GSC-derived intrancranial xenograft tumors. Red arrows indicate tumors. **(O)** IB analysis of USP9X, CD44 and OLIG2 in MES 21, MES 505, PN 35 and 182 GSCs. **(P)** IB analysis of USP9X and ALDH1A3 in PN 35 and 182 GSCs transduced with USP9X or vector control. **(Q)** qRT-PCR analysis of ALDH1A3 mRNA expression in MES 21 and 505 GSCs depleted of endogenous USP9X by two independent shRNA. **(R)** qRT-PCR analysis of ALDH1A3 mRNA expression in PN 35 and 182 GSCs after transduction with vector control or Flag-USP9X. Scale bars: 500 μm **(H** and **I)**, 25 μm **(L** and **M)**, 1 mm **(N).** Data in **(D, E, Q** and **R)** are means ± SD of three independent experiments. 1-way ANOVA with Dunnett's post-test for **(D, Q** and **R)**, 2-tailed Student's *t* test for **(E)**.

Supplemental Figure 2. USP9X interacts with ALDH1A3

(A) NHAs were transfected with His-ALDH1A3 alone or in combination with Flag-tagged USP9X WT or USP9X C1566A, and cell lysates were analyzed by IP with Flag beads followed by IB with antibodies against His and Flag. **(B)** Cell lysates from U87MG and T98G were analyzed by IP using antibodies against USP9X and ALDH1A3, and then subjected to IB analysis. IgG was used as the isotype control.

Supplemental Figure 3. High USP9X expression predicts enrichment of ALDH1A3^{high} MES GSCs with potent tumorigenic capability

(A and **B)** Kaplan-Meier survival curves of mice implanted with indicated number of USP9X^{high} or USP9X^{low} subpopulations isolated from MES 21 **(A)** and 505 **(B)** GSCs (n = 8). ****P<0.0001 by log-rank (Mantel-Cox) test.

Supplemental Figure 4. Ablation of USP9X expression impairs the self-renewal, tumorigenicity and radio/chemoresistance of MES GSCs

(A and **B)** Representative images of EdU incorporation assays **(A)** and quantification of EdU-positive cells **(B)** in MES 21 and 505 GSCs transduced with shCtrl or shUSP9X, reconstituted with vector control or ALDH1A3. Cells in green represent EdU-positive cells. Nuclei were counterstained with DAPI (blue). **(C** and **D)** Representative BLI of intracranial GBM xenografts derived from luciferase-labeled MES 21 **(C)** and 505 **(D)** GSCs with indicated modifications. Colored scale bars represent photons/sec/cm2/steradian. **(E)** IB analysis of USP9X in PN 35 and 182 GSCs transduced with USP9X or vector control. **(F** and **G)** Primary neurosphere formation was assessed in PN 35 and 182 GSCs transduced with USP9X or vector control, in response to IR (5Gy) **(F)** or TMZ (100 μM) **(G)**. **(H)** IB analysis of USP9X in USP9X-overexpressing PN 35 and 182 GSCs transduced with shUSP9X or shCtrl. **(I** and **J)** Primary neurosphere formation was assessed in USP9X-overexpressing PN 35 and 182 GSCs transduced with shUSP9X or shCtrl, in response to IR (5Gy) **(I)** or TMZ (100 μM) **(J)**. Data in **(B, F, G, I** and **J)** are means ± SD of three independent experiments. ***P<0.001 by 2-tailed Student's t test.

Supplemental Figure 5. Pharmacological inhibition of USP9X attenuates the tumor-initiating ability of MES GSCs with high ALDH1A3 activity

(A) qRT-PCR analysis of ALDH1A3 mRNA expression in MES 21 and 505 GSCs following treatment with 1 μM WP1130 for 24 hours. **(B** and **C)** Cell growth rates **(B)** and EdU incorporation **(C)** in MES 21 and 505 GSCs after treatment with 1 μM WP1130 for 24 hours. Data are shown as means ± SD. $^{**}P < 0.01$.$^{***}P < 0.001$. **(D)** Kaplan-Meier survival curves of mice intracranially injected MES 21 and 505 GSCs after treatment with 25 mg/kg WP1130 or vehicle (n = 8). $^{****}P<0.0001$ by log-rank (Mantel-Cox) test. Data in **(A-C)** are means ± SD of three independent experiments. $^{**}P<0.01$, $^{***}P<0.001$ by 2-tailed Student's *t* test.

Supplemental Figure 6. USP9X shows a positive correlation with ALDH1A3 protein levels and is associated with poor survival of ALDH1A3^{high} MES GBMs

(A) Correlations of IHC staining data for high or low USP9X expression relative to level of ALDH1A3 are shown. (*P* values by Kendall's tau-beta). **(B)** Schematic illustration of the USP9X -mediated ALDH1A3 stabilization and MES maintenance in GSCs. USP9X reverses ALDH1A3 polyubiquitylation and protects ALDH1A3 from proteasomal degradation, which lead to the stabilization and accumulation of ALDH1A3, thereby resulting in the maintenance of MES features of GSCs. These effects can be effectively abrogated by the USP9X inhibitor WP1130.

Supplemental Table 1. Patient-derived GSC inventory

Cell Line Name	GSC subtype	Pathological Diagnosis	Clinical Status
21	Mesenchymal	Glioblastoma, WHO IV	Primary
505	Mesenchymal	Glioblastoma, WHO IV	Primary
35	Proneural	Glioblastoma, WHO IV	Primary
182	Proneural	Glioblastoma, WHO IV	Primary

Supplemental Table 2. STR analysis of cell lines used for this study

	U87MG	T98G	MES 21	MES 505	PN 35	PN 182
Amelogenin	X, Y	X, Y	X	X, Y	X	X
CSF1PO	10, 11	10, 12	12	10, 12	11, 12	9, 12
D13S317	8, 11	13	8, 13	10, 13	10, 11	8, 11
D16S539	12	13	11, 13	9	9, 11	11, 12
D5S818	11, 12	10, 12	12	11, 13	12, 13	12, 13
D7S820	8, 9	9, 10	9, 10	9, 11	8, 9	8, 11
THO1	9.3	7, 9.3	6, 9.3	6, 9.3	9.3	9
TPOX	8	8	9, 11	8, 11	8, 11	9
vWA	15,17	17, 20	14, 19	15, 17	15, 16	16, 17

Supplemental Table 3. Characterization of the sequences of shRNAs and cDNA primers

Sequences for shRNAs and cDNA primers	
TRC shRNA Control	N/A
USP9X shRNA #1	ATTCACAGCTTTGAAGAATCG
USP9X shRNA #2	TAATGTCTACGTTTAGGGTCG
ALDH1A3-Forward	TCTCGACAAAGCCCTGAAGT
ALDH1A3-Reverse	TATTCGGCCAAAGCGTATTC

Supplemental Figure 1

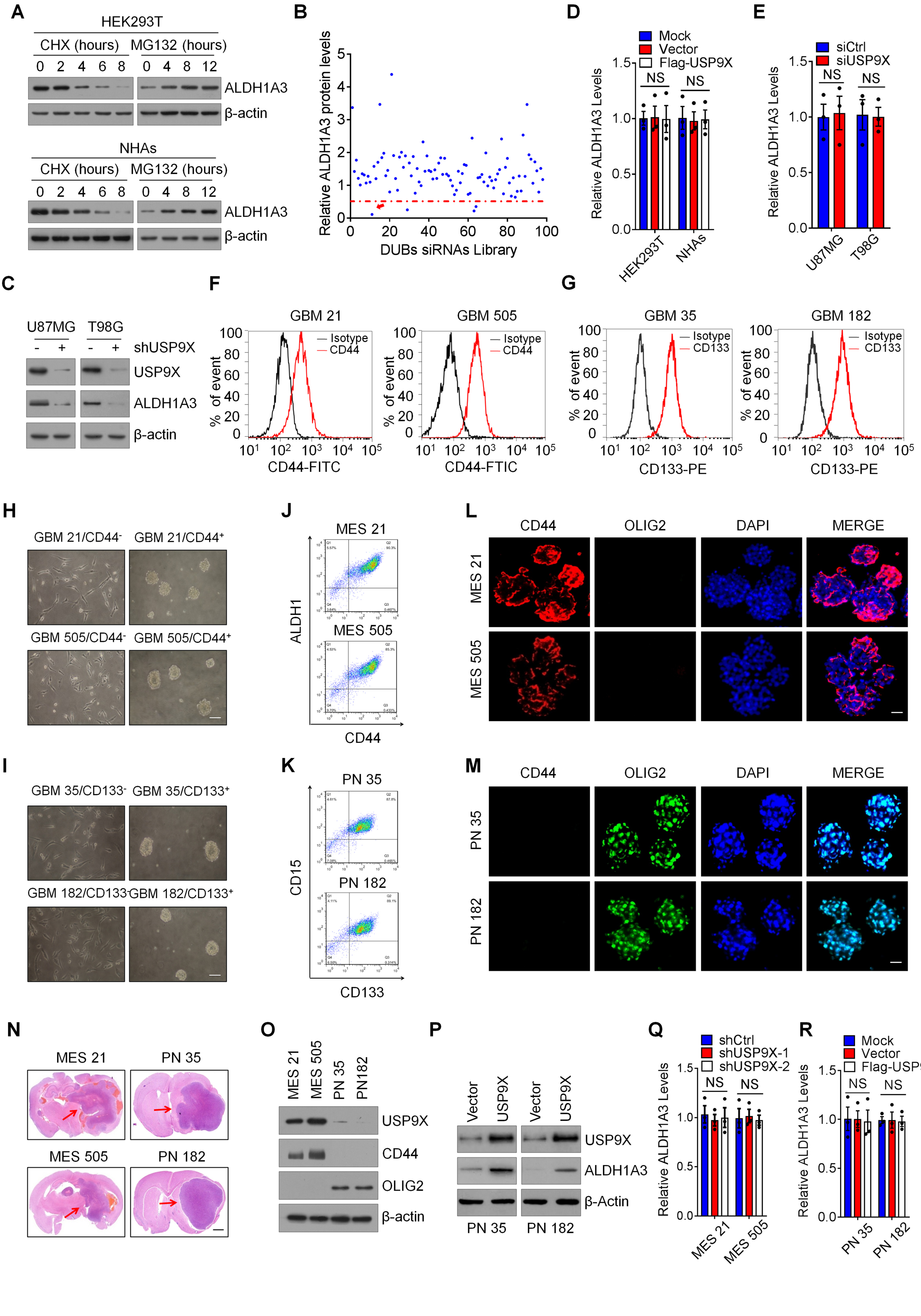

Supplemental Figure 2

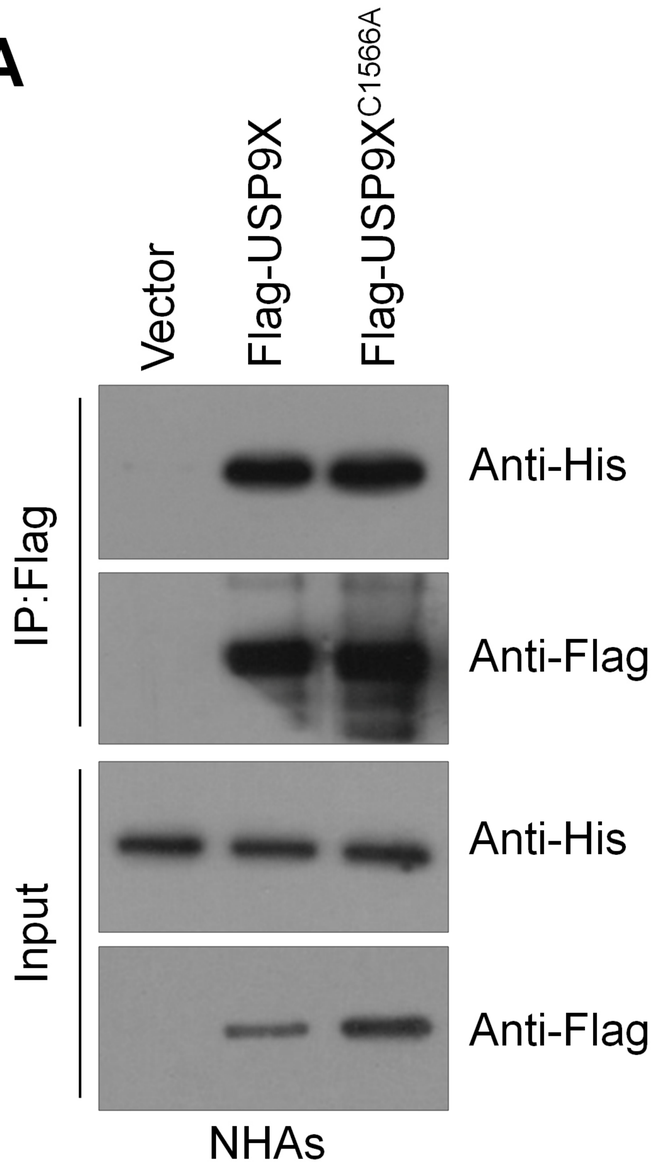

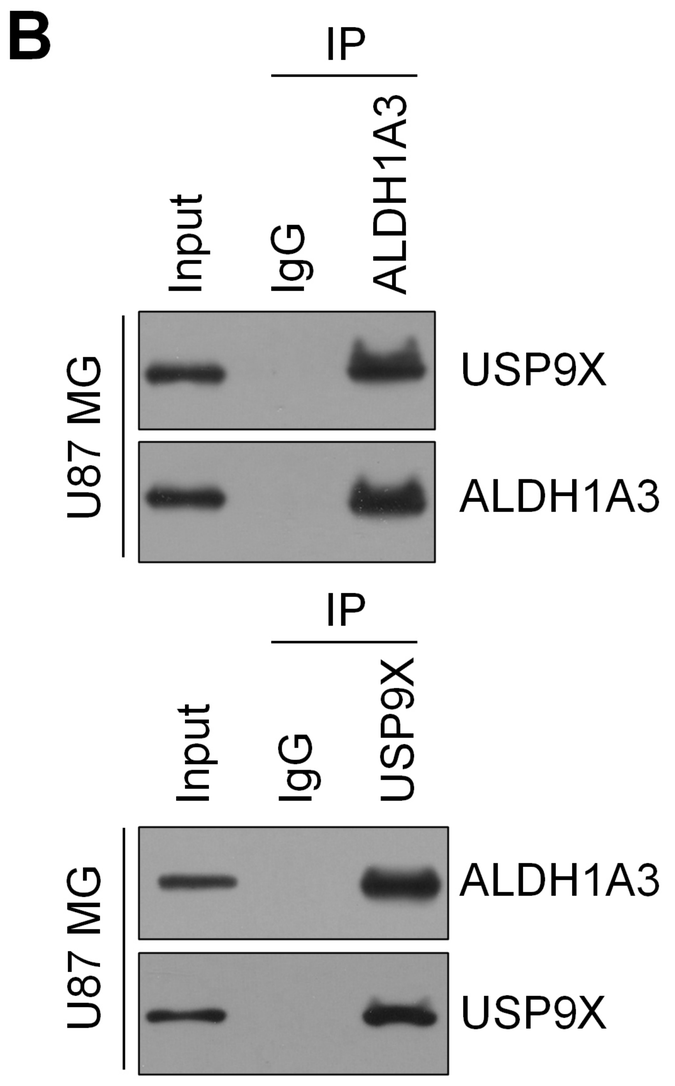

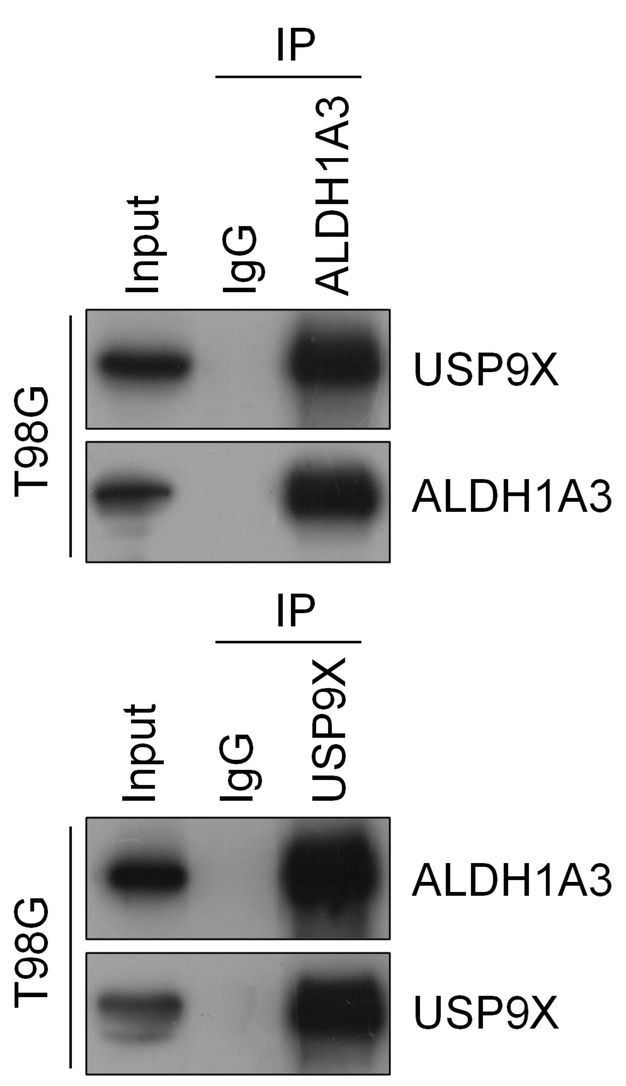

Supplemental Figure 3

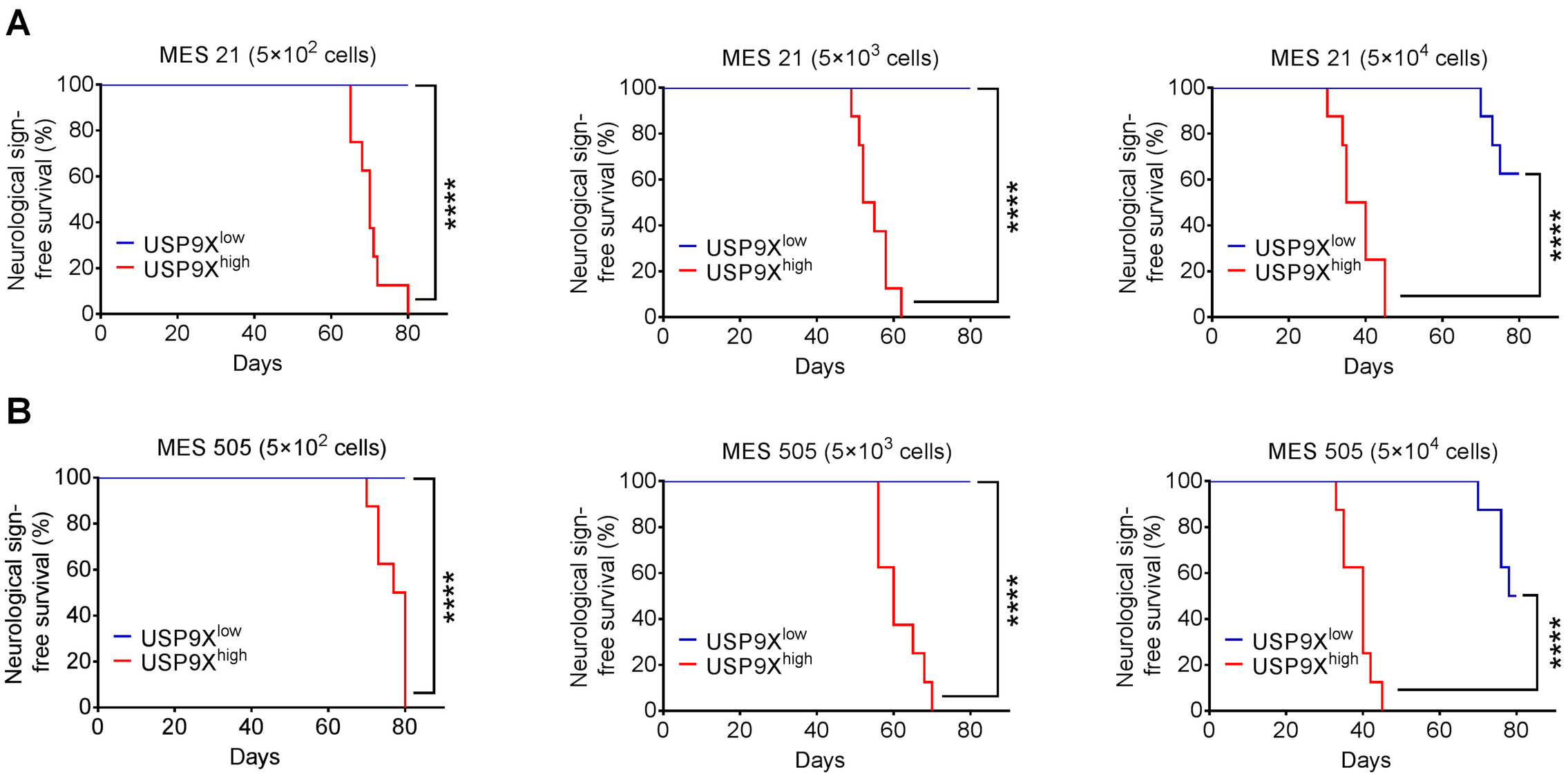

Supplemental Figure 4

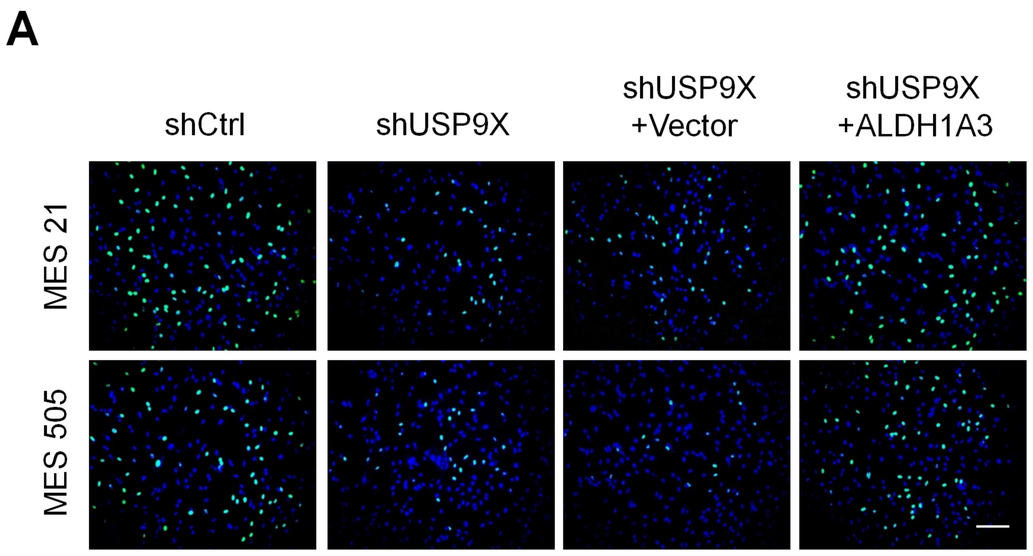

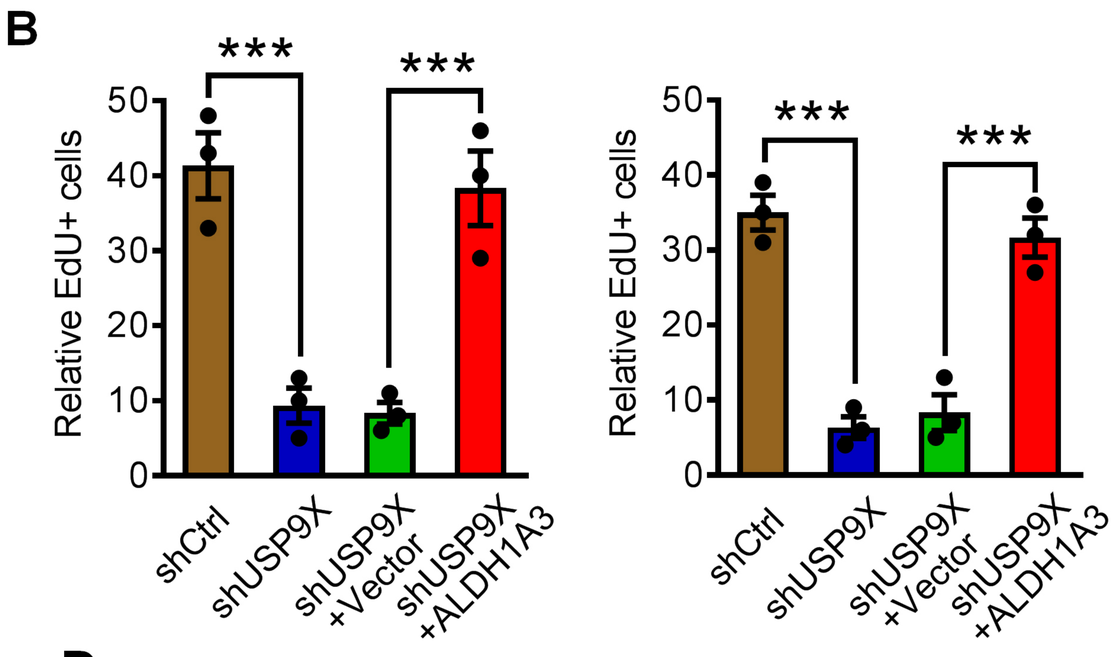

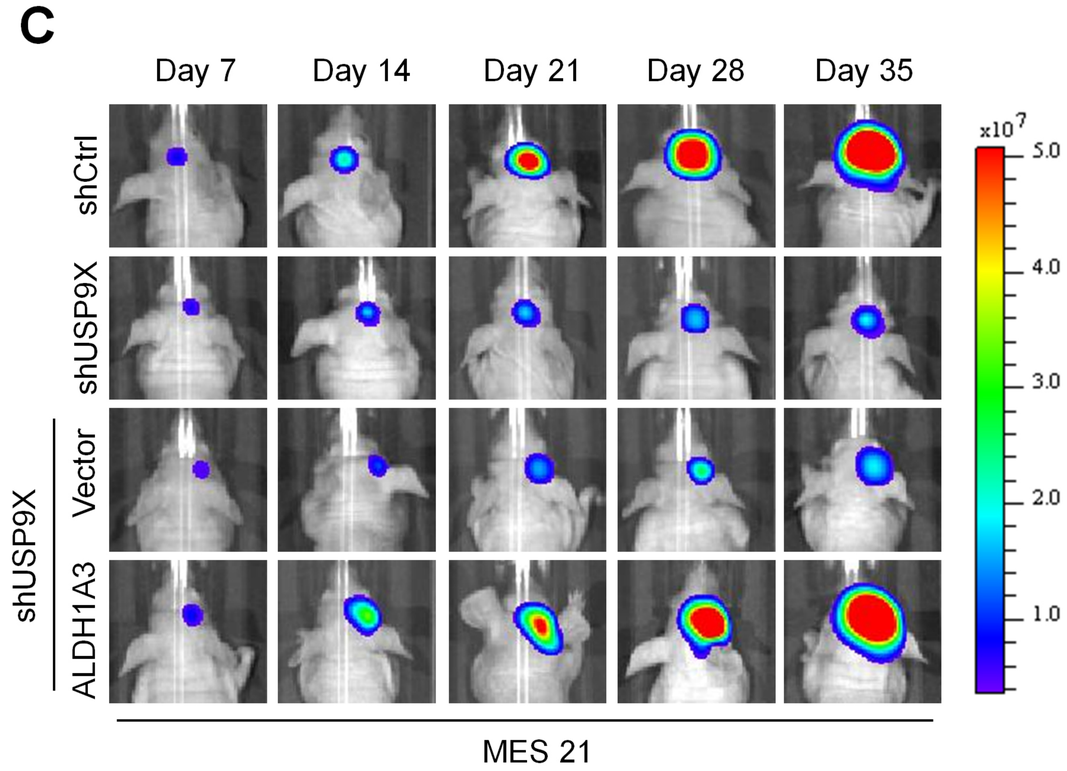

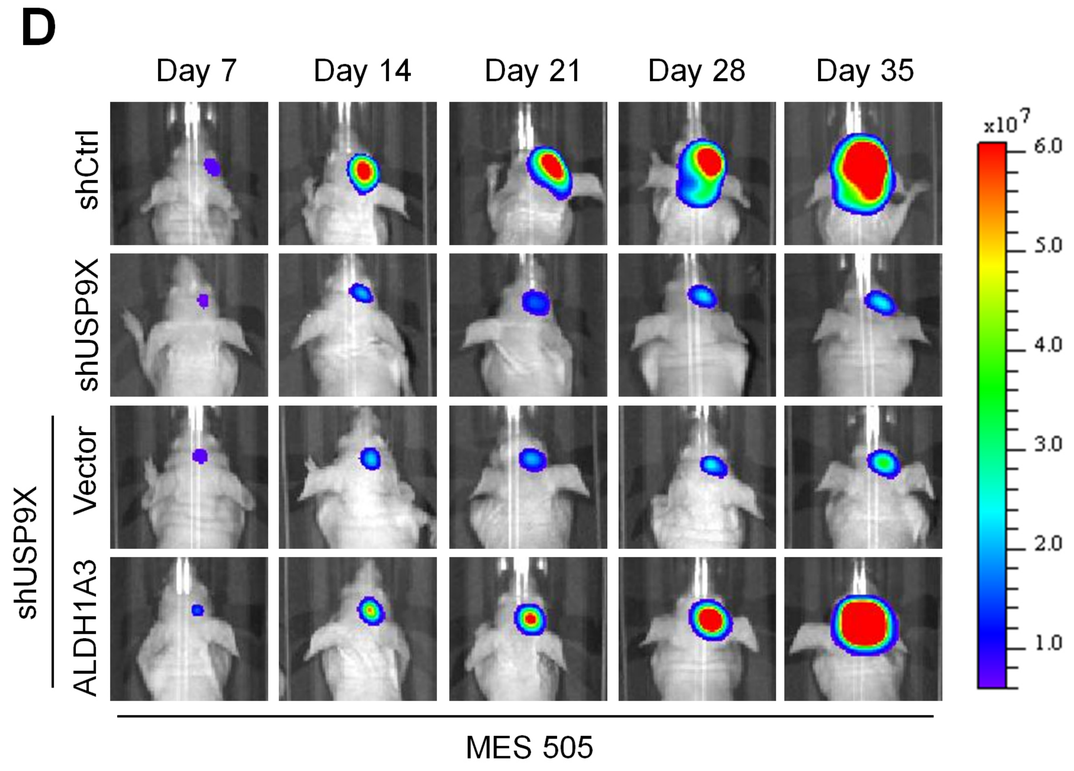

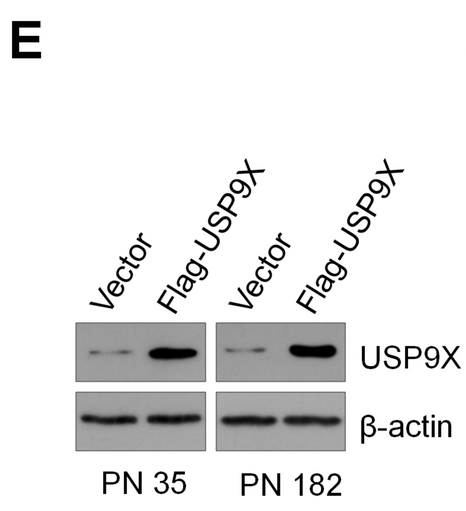

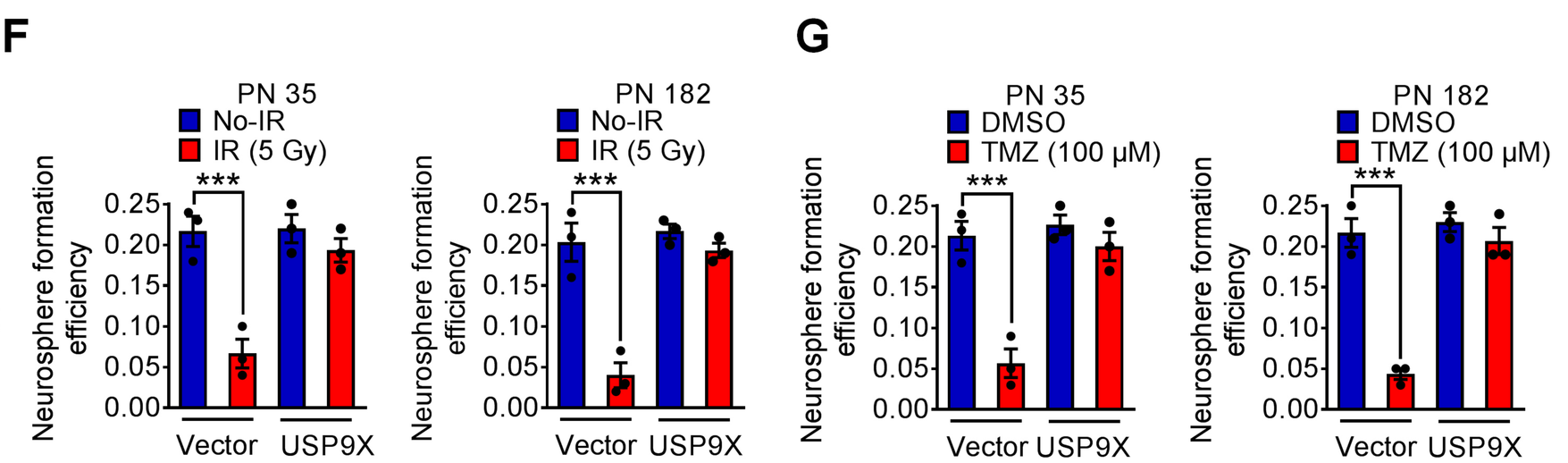

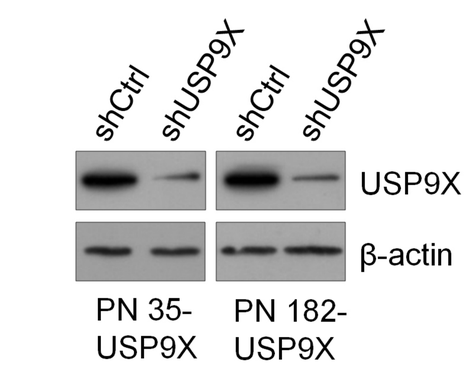

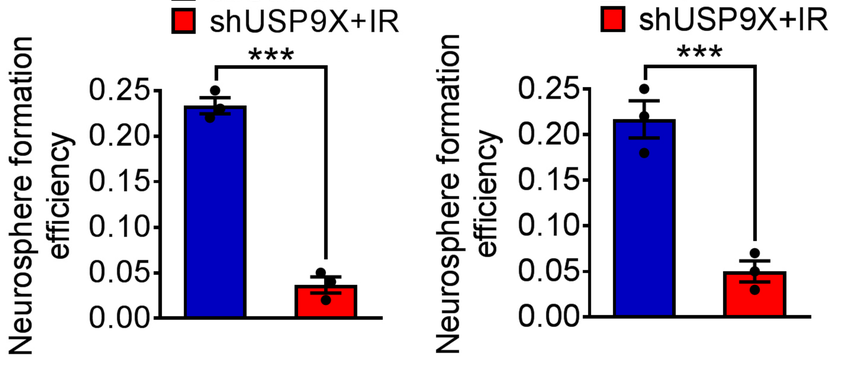

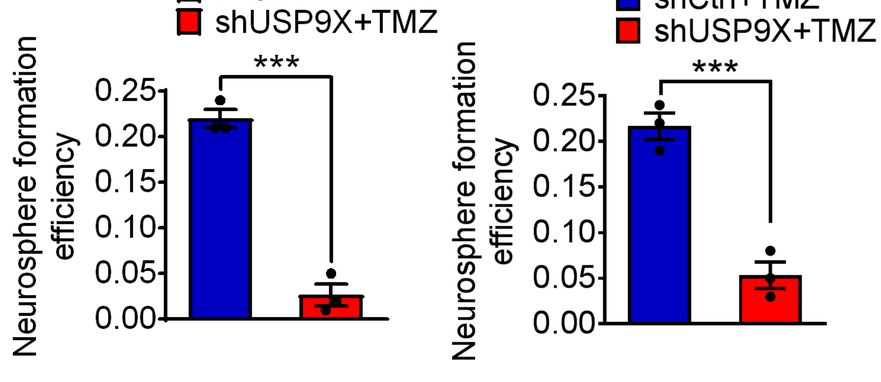

Supplemental Figure 5

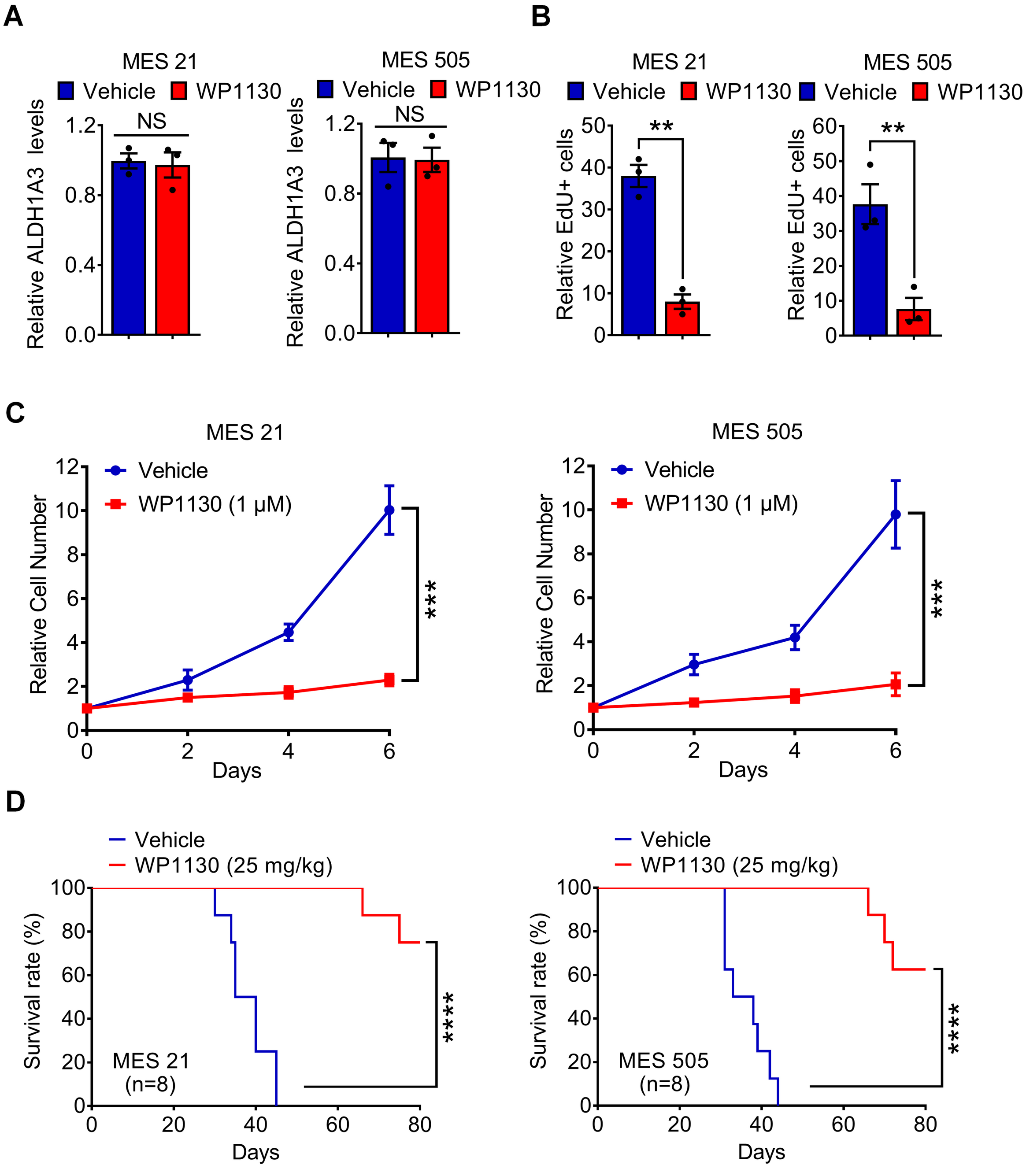

Supplemental Figure 6